STEM CELLS®

Bone marrow-derived myeloid progenitors in the leptomeninges of adult mice

Tobias Koeniger[1] | Luisa Bell[1] | Anika Mifka[2] | Michael Enders[2] |
Valentin Hautmann[1] | Subba Rao Mekala[1] | Philipp Kirchner[3] | Arif B. Ekici[3] |
Christian Schulz[4] | Philipp Wörsdörfer[1] 🆔 | Stine Mencl[5] |
Christoph Kleinschnitz[5] | Süleyman Ergün[1] | Stefanie Kuerten[1,2,6] 🆔

[1]Institute of Anatomy and Cell Biology, Julius Maximilian University of Würzburg, Würzburg, Germany

[2]Institute of Anatomy and Cell Biology, Friedrich-Alexander University Erlangen-Nürnberg, Erlangen, Germany

[3]Institute of Human Genetics, University Hospital Erlangen, Friedrich-Alexander University Erlangen-Nürnberg, Erlangen, Germany

[4]Medizinische Klinik und Poliklinik I, Ludwig Maximilian University of Munich, Munich, Germany

[5]University Hospital Essen, Department of Neurology, University Duisburg-Essen, Essen, Germany

[6]Anatomisches Institut, Neuroanatomie, Rheinische Friedrich-Wilhelms-Universität Bonn, Bonn, Germany

Correspondence
Stefanie Kuerten, MD, PhD, Anatomisches Institut, Neuroanatomie, Rheinische Friedrich-Wilhelms-Universität Bonn, 53115 Bonn, Germany.
Email: stefanie.kuerten@uni-bonn.de

Abstract

Although the bone marrow contains most hematopoietic activity during adulthood, hematopoietic stem and progenitor cells can be recovered from various extramedullary sites. Cells with hematopoietic progenitor properties have even been reported in the adult brain under steady-state conditions, but their nature and localization remain insufficiently defined. Here, we describe a heterogeneous population of myeloid progenitors in the leptomeninges of adult C57BL/6 mice. This cell pool included common myeloid, granulocyte/macrophage, and megakaryocyte/erythrocyte progenitors. Accordingly, it gave rise to all major myelo-erythroid lineages in clonogenic culture assays. Brain-associated progenitors persisted after tissue perfusion and were partially inaccessible to intravenous antibodies, suggesting their localization behind continuous blood vessel endothelium such as the blood-arachnoid barrier. *Flt3*^Cre lineage tracing and bone marrow transplantation showed that the precursors were derived from adult hematopoietic stem cells and were most likely continuously replaced via cell trafficking. Importantly, their occurrence was tied to the immunologic state of the central nervous system (CNS) and was diminished in the context of neuroinflammation and ischemic stroke. Our findings confirm the presence of myeloid progenitors at the meningeal border of the brain and lay the foundation to unravel their possible functions in CNS surveillance and local immune cell production.

KEYWORDS
hematopoietic, meninges, mouse, myeloid, progenitor

1 | INTRODUCTION

Adult hematopoiesis primarily takes place in the bone marrow (BM). Here, a small pool of self-renewing hematopoietic stem cells (HSC) feeds into a proliferative hierarchy of increasingly committed progenitors, which eventually differentiate into myeloid and lymphoid cell types to compensate for mature cell turnover. Hematopoiesis is a dynamic process, which repeatedly changes its site during development. First, hematopoietic activity emerges in the yolk sac (YS) and later transitions to the fetal liver, until adult hematopoiesis in the BM is eventually established.[1]

Even during adulthood, hematopoietic stem and progenitor cells (HSPC) retain a certain degree of mobility. A small fraction of HSPCs constantly recirculates between BM and peripheral blood[2] and can be recovered from various extramedullary sites such as the spleen,[3] liver,[4] muscle,[5] lungs,[6] intestine,[6,7] kidneys,[6] thymus,[8] and aorta.[9,10] It has originally been proposed that the continuous trafficking of HSPCs is a mechanism to maintain full occupancy of HSPC niches in all BM cavities.[2] Now, we know that on their journey, HSPCs surveil extramedullary sites and participate in local immune responses.[11] They sense pathogens through pattern recognition receptors,[12-14] are recruited to sites of injury,[11,15] and react to inflammatory stimuli with proliferation,[11,16,17] differentiation into myeloid cells,[11,12] as well as with secretion of chemokines and cytokines.[18]

A multitude of studies on the maintenance of microglia unintentionally demonstrated that HSPCs also engraft the brain following tissue damage by irradiation or chemotherapy, where they differentiate into microglia-like cells.[19-22] Similarly, HSPCs seem to be recruited from the BM to the central nervous system (CNS) during experimental cerebral ischemia, where they might limit the infarct volume.[23] However, it is not entirely clear whether the CNS harbors HSPCs under steady-state conditions. HSPC-like cells have been recovered from the healthy adult brain with varying success,[11,24-27] but their nature and localization remain insufficiently defined.

Here, we describe a heterogeneous population of myeloid progenitors in the leptomeninges (LM) of adult mice that was derived from adult BM and differentiated into all major myelo-erythroid cell lineages in vitro. Their occurrence was linked to the immunologic state of the CNS and was diminished in experimental autoimmune encephalomyelitis (EAE) and ischemic stroke. As ever more functions of HSPCs in the immune system are unraveled, the presence of myeloid progenitors at the adult CNS interfaces may have broad implications for neuroinflammation and -infection.

2 | MATERIALS AND METHODS

2.1 | Mice

C57BL/6J, B6.Iba1-GFP,[28] Flt3[Cre],[29] R26[mT/mG],[30] and B6.ubc-GFP[31] mice were maintained and bred at the facilities of the Centre for Experimental Molecular Medicine (Würzburg, Germany) or purchased from Charles River Laboratories. Heterozygous B6.Cx3cr1-GFP mice[32] were kindly provided by Andreas Beilhack (Medizinische Klinik

Significance statement

Hematopoiesis usually takes place in the bone marrow. Yet, stem and progenitor cells regularly leave their niche to circulate throughout the body, where they can actively participate in immune responses. Intriguingly, hematopoietic progenitor-like cells have even been reported in brain homogenates of mice, but their nature, origin, and location remain insufficiently defined. In contrast to the brain parenchyma, this study places the leptomeningeal barrier of the brain among an array of tissues, which are constantly patrolled by progenitors from the bone marrow. As ever more functions of these cells in immunity are unraveled, data of this study will provide new impulses for neuroimmunological research.

und Poliklinik II & Universitäts-Kinderklinik, Julius Maximilian University of Würzburg, Würzburg, Germany). Animals were housed in a pathogen-free, temperature- and humidity-controlled environment with a 12-hour light cycle and given ad libitum access to food and water. Male and female mice were used in experiments at 10 to 18 weeks of age. All procedures were performed in accordance with the *German Animal Welfare Act* and the *Guide for Care and Use of Laboratory Animals*,[33] and were approved by the government of lower Franconia, Germany (approval number: 55.2 DMS-2532-2-109) or the "Landesamt für Natur, Umwelt- und Verbraucherschutz Nordrhein-Westfalen" (approval number: 81-02.04.2018.A285).

2.2 | Preparation of single cells from adult tissues

A detailed procedure is provided in Supplementary Method S1. In brief, mice were sacrificed and transcardially perfused with heparinized PBS. Mixed peripheral blood was collected during perfusion. Femora/tibiae, skull, and spleen were flushed or crushed in PBS. Brain, liver, kidney, and heart were minced and digested with collagenase/dispase at 37°C for 60 minutes. If not stated otherwise, brain tissue included parenchyma, choroid plexus, and LM. Myelin/debris was removed from brain isolates via centrifugation in 20% BSA in PBS. Erythrocytes were removed from all preparations via treatment with AMC lysis buffer.

2.3 | Colony-forming unit (CFU) assay

A detailed procedure is provided in Supplementary Method S2. In brief, live cells were counted using a hemocytometer and trypan blue, before seeding defined cell quantities in collagen- or methylcellulose-based media, supplemented with hematopoietic growth factors (SCF, IL-3, TPO, EPO, GM-CSF, IL-34 or SCF, IL-3, IL-6, EPO, respectively). Cultures were incubated for 7 to 10 days, before cell colonies (>30 cells) were counted manually at an inverted microscope. Morphologic

features that were used to differentiate colony types are listed in Table S1.

2.4 | Flow cytometry and cell sorting

A detailed procedure is provided in Supplementary Method S3. In brief, cells were stained with antibodies for 10 minutes at 2°C to 8°C, before cell sorting was performed at a FACSAria III cell sorter (BD Biosciences), equipped with a 70 μm nozzle. All reagents used are listed in Table S2. Data were analyzed using FlowJo software (Tree Star). Representative dot plots shown in the figures are contour plots with 5% contour levels including outliers. Gating strategies usually included upstream steps to select for single, viable cells based on FSC/SSC characteristics and DAPI exclusion. As sorted cells were counted in trypan blue prior to CFU assays, DAPI staining was omitted during sorts.

2.5 | Antibody injections

Mice were injected into the tail vein with 5 or 10 μg of αCD45 allophycocyanin (APC; BioLegend, #559864) diluted in 100 μL of sterile, heparinized (500 U/mL) PBS -Ca^{2+}/Mg^{2+}. Mice were sacrificed after a circulation time of 5 or 60 minutes. Each injected mouse was checked for sufficient staining of blood leukocytes (>90% positive cells) or skull BM cells (>60% positive cells). Insufficiently labeled animals were excluded from the experiment.

2.6 | Pappenheim staining

Cytospin samples were air-dried, fixed in methanol for 10 minutes at room temperature, and successively stained with May-Grünwald solution (Sigma-Aldrich, #63590) and Giemsa-Stain, modified solution (Sigma-Aldrich, #48900-1L-F).

2.7 | BM transplantation

BM chimeric mice were generated using αCD45-saporin (CD45-SAP) as previously described.[34] In brief, female C57BL/6J mice at the age of 8 weeks were injected into the tail vein with CD45-SAP at 3 mg/kg body weight, diluted in 200 μL sterile PBS. CD45-SAP was prepared by mixing biotinylated αCD45 antibody (clone 104, BioLegend, #109804) with streptavidin-ZAP (Advanced Targeting Systems, #IT-27) at an equimolar ratio. The mixture was incubated for 30 minutes at room temperature, before adding PBS to achieve the desired concentration for injection. Four days later, BM cells were prepared by flushing femora and tibiae of gender-matched B6.ubc-GFP mice. Total cellularity was determined by complete blood cell counting using a hemocytometer and trypan blue. Eventually, 10^7 BM cells in 200 μL sterile PBS were injected into the tail vein of preconditioned mice.

2.8 | Meningeal whole-mounts

Dissection and immunostaining of mouse whole-mount meninges was performed as previously described.[35] In brief, mice were euthanized and transcardially perfused with ice-cold PBS, before fixation of the dorsal skull cap with 4% paraformaldehyde in PBS at room temperature for 60 minutes. The meninges were gently removed from the skull under a dissecting microscope, permeabilized with 0.1% Triton X-100 and 0.05% Tween-20, and stained with anti-c-KIT antibody (Thermo Fisher Scientific, #14-1171-81, 1:300) and avidin-FITC (BioLegend, #405101, 1:200) overnight at 4°C. After washing, meninges were incubated with Cy3-conjugated AffiniPure goat anti-rat IgG (H + L) (Jackson ImmunoResearch Laboratories Inc, #112-165-003) and 1 μg/mL DAPI at room temperature for 60 minutes. Eventually, meninges were mounted using mowiol mounting solution and analyzed at a confocal microscope. The density of stained cells was estimated by manual counting of 10 individual images per sample (approximately 0.4 mm^2 per image), which were selected at random.

2.9 | Single cell RNA sequencing

The detailed procedure is provided in Supplementary Method S6.

2.10 | Experimental autoimmune encephalomyelitis

For the induction of EAE, mice were immunized with MP4 antigen as previously described.[36] In brief, male C57BL/6J mice at the age of 10 to 16 weeks were injected subcutaneously into both flanks with a total dose of 200 μg MP4 antigen (Alexion Pharmaceuticals, Cheshire, Connecticut), emulsified in complete Freund's adjuvans (CFA). An intraperitoneal injection of 200 ng pertussis toxin (List Biological Laboratories, Hornby, Ontario, Canada; Cat #181) in PBS was given at the day of immunization and 48 hours later. Mice were sacrificed for analysis during the chronic stage of disease, 43 to 66 days after immunization.

2.11 | In vivo MCAO ischemia model

Male C57BL/6N mice aged 10 to 12 weeks were subjected to right sided middle cerebral artery occlusion (MCAO) followed by 1 to 3 days of reperfusion. Focal cerebral ischemia was induced by 30 minutes transient middle cerebral artery occlusion (tMCAO) as previously described.[37,38] Mice were anesthetized with 2.5% isoflurane in O_2 (Abbott). Core body temperature was maintained at 37°C throughout surgery by using a feedback-controlled heating device. Following a midline skin incision in the neck, the proximal common carotid artery and the external carotid artery were ligated and a standardized silicon rubber-coated 6.0 nylon monofilament (6023910PK10; Doccol) was

inserted and advanced via the right internal carotid artery to occlude the origin of the right MCA. The intraluminal suture was left in situ for 30 minutes. The animals were then reanesthetized and the occluding monofilament was withdrawn to allow for reperfusion. Operation time per animal did not exceed 10 minutes and all animals underwent post-surgical pain management (one bolus of 0.1 mg/kg intraperitoneal injected buprenorphine 30 minutes before surgery and daily for 3 days 5 mg/kg subcutaneous carprofen, both mixed in sterile saline). After the abovementioned reperfusion time, all animals were transcardially perfused with PBS after an overdose of intraperitoneally injected ketamine-xylazine solution (more than 0.2 mg/kg ketamine and 0.01 mg/kg xylazine in saline).

2.12 | Statistical analysis and software

Statistics were performed using GraphPad Prism version 6.01 for Windows, GraphPad Software (La Jolla, California, www.graphpad. com). Values given in the text represent mean ± SD. Applied statistical tests are described in the figure legends. Images were analyzed using Fiji.[39]

3 | RESULTS

3.1 | Rare colony-forming cells were detected in whole brain homogenates of adult mice

Adult mice were sacrificed and transcardially perfused to remove intravascular cells. Single cell suspensions were prepared from hema-topoietic (BM, blood, liver, spleen) and nonhematopoietic tissues (brain, heart, kidney) and analyzed in collagen-based colony-forming unit (CFU) assays (Figure 1A). As expected, cell colonies formed at high frequency in BM samples taken from femur/tibia (373 ± 66 per 10^5 cells) or skull (482 ± 109 per 10^5 cells) and could also be observed in the spleen (15 ± 4 per 10^5 cells) and liver (12 ± 3 per 10^5 cells) (Figure 1B). In the adult brain (parenchyma + choroid plexus + LM), 7 ± 4 colony-forming units-culture (CFU-C) per 10^5 cells were detected, which by trend was more than the frequency of CFU-Cs among leukocytes from mixed peripheral blood (4 ± 3 per 10^5 cells). The brain seemed to harbor more CFU-Cs than other nonhematopoietic organs tested, as heart cells only gave rise to <1 CFU-Cs per 10^5 cells and no CFU-Cs were detected in the kidney.

3.2 | CFU-Cs were sequestered inside the CNS and did not express markers of self-renewing microglia or border macrophages

During brain dissection, the cranium was opened with scissors expos-ing skull BM, which naturally harbors a high frequency of CFU-Cs (Figure 1B). We calculated that a spill of ~10^4 BM cells would suffice to explain the CFU-C frequencies observed within brain cell suspensions. To exclude such contamination, CNS tissue was extracted through the foramen magnum, this way conferring minimal damage to the skull, and analyzed in CFU assays (Figure S1). With this procedure, we were able to detect a similar amount of CFU-Cs in the recovered whole brain homogenates, making it unlikely that BM spill accounted for the observed colony formation.

We also considered other potential sources of brain-derived CFU-Cs: residual circulating HSPCs and resident macrophages (or a subpopulation thereof).

Microglia and most CNS border macrophages have been shown to self-renew within the adult mouse brain[40,41] and have demon-strated an extensive proliferative capacity in genetic and pharmaco-logical repopulation models.[42-44] As our CFU assay included factors that act on macrophages/microglia,[45-48] the latter might have been stimulated to form cell colonies in vitro.

Also, HSPCs are constantly circulating in blood and thus are pre-sent inside the CNS vascular system. Although perfusion clears most blood from tissues, it cannot eliminate all intravascular cells (notice-able by residual erythrocytes in cell isolates), especially those that are interacting with the vessel endothelium.[49] Therefore, we injected mice intravenously (i.v.) with fluorescently labeled αCD45 antibody to tag intravascular CD45$^+$ cells (IV-CD45) in vivo (Figure 1C). Injecting 5 μg of antibody sufficed to stain >99% of all leukocytes in mixed peripheral blood within 5 minutes. Increasing the antibody amount and circulation time (10 μg, 60 minutes) led to efficient penetration of antibody through the fenestrated endothelium of skull BM, addition-ally staining >80% of BM cells. Importantly, tissue processing (enzy-matic digestion and myelin removal) did not remove antibody labeling (Figure S2).

We used B6.Iba1-GFP mice in our injection experiments, in which microglia and CNS border macrophages are endogenously tagged via expression of green fluorescent protein (GFP).[28] This strategy allowed us to simultaneously assess the contribution of mature macrophages, skull BM, and sequestered intravascular cells to colony formation. IV-CD45$^-$ (= tissue resident) cells, were FACS-sorted from brain sus-pensions, separated into GFP$^+$ macrophages and GFP$^-$ "non-macrophage" populations (Figure 1D), and analyzed via CFU assays (Figure 1E). At day 7 of culture, colonies were solely contained in GFP$^-$ fractions, showing that mature macrophages did not contribute to colony-formation. Compared to noninjected controls, colony fre-quency was lowered by around 50% in sorted samples of mice that had been injected with αCD45 antibody. This indicated that some of the brain-associated CFU-Cs were accessible to intravenous antibody and therefore were removed during the sort. However, there was no difference between the two antibody injection regimens (staining pre-dominantly blood, or equally blood and BM). This demonstrated that the nonremovable CFU-Cs were not the result of BM contamination, but were located behind the blood-brain or blood-arachnoid barriers.

As most research on the self-renewal of mature brain macro-phages is based on Cx3cr1 lineage tracing,[43,44] we wanted to exclude the possibility that a proliferative Iba1$^-$ Cx3cr1$^+$ microglia/macro-phage subpopulation was present in brain isolates. To this end, we sorted GFP$^+$ and GFP$^-$ cells from the brains of B6.Cx3cr1-GFP$^{+/-}$
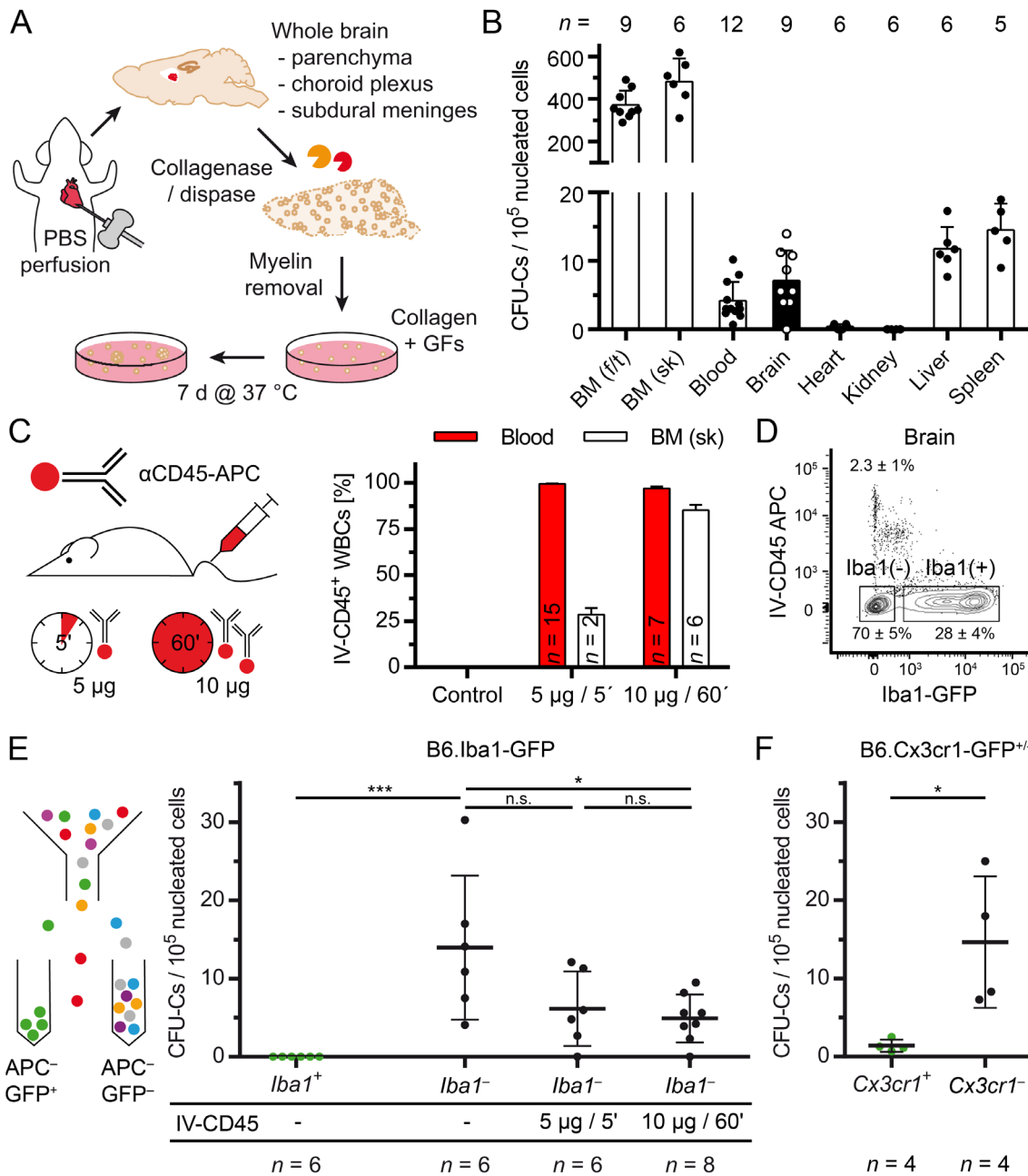
FIGURE 1 Colony-forming units-culture (CFU-C) in whole brain homogenates of adult mice. A, Schematic overview of the experimental procedure to quantify CFU-Cs in brain suspensions. GF, growth factors. B, CFU-Cs were detected in different adult hematopoietic and nonhematopoietic tissues including the brain. Data represent mean + SD and were pooled from at least two independent experiments including a total of n = 5-12 mice. BM, bone marrow; f/t, femur/tibia; sk, skull. C, In order to label intravascular and BM-resident cells, mice were injected intravenously (i.v.) with αCD45-APC antibody. A dosage of 5 μg efficiently stained circulating white blood cells (WBCs) within a circulation time of 5 minutes, as determined by flow cytometry. An increased dosage (10 μg) and circulation time (60 minutes) additionally stained >80% of nucleated skull BM cells. Data represent mean + SD. BM (sk), skull bone marrow. D, Following i.v. injection of αCD45-APC antibody, brain cell suspensions of B6.Iba1-GFP mice could be separated into APC⁻ GFP⁺ resident macrophages and APC⁻ GFP⁻ "nonmacrophage" cells via cell sorting, as shown in the representative dot plot. E, Brain-derived CFU-Cs were retained within the GFP⁻/*Iba1*⁻ "nonmacrophage" fraction. Removal of intravenously stained CD45⁺ cells (IV-CD45) lowered the frequency of CFU-Cs in the GFP⁻/*Iba1*⁻ fraction, but did not eliminate clonogenic activity. Brain cell suspensions were prepared from B6.Iba1-GFP mice previously injected with αCD45-APC antibody as described in (C). Cells were sorted based on APC and GFP fluorescence as shown in (D), before analyzing the fractions in collagen-based CFU assays. Colonies were counted on day 7 of culture. Data represent mean ± SD and are the summary of at least two independent experiments, including a total of n = 6-8 mice per group. Statistical analysis was performed using ordinary one-way ANOVA with Tukey's multiple comparisons test. *P < .05, ***P < .001; n.s., nonsignificant. F, Brain-derived CFU-Cs predominantly resided in the *Cx3cr1*⁻ fraction. Brain cell suspensions were prepared from B6.Cx3cr1-GFP⁺/⁻ mice. Cells were sorted based on GFP fluorescence into *Cx3cr1*⁻ and *Cx3cr1*⁺ fractions, which were individually analyzed in collagen-based CFU assays. Colonies were counted on day 7 of culture. Data are given as mean ± SD and are representative of two independent experiments, each including n = 4 mice. Statistical analysis was performed using an unpaired t test. *P < .05

reporter mice (Figure 1F). Unlike Iba1-GFP$^+$ cells, Cx3cr1-GFP$^+$ cells rarely gave rise to relatively small colonies in CFU assays (1.4 ± 0.8 per 10^5 cells; Figure S3). Still, the GFP$^-$ "nonmacrophage" fraction contained 10-times more colony-forming activity (14.7 ± 8.4 per 10^5 cells), corroborating that clonogenicity was not due to proliferation of macrophages/microglia.

3.3 | Brain-associated CFU-Cs comprised a heterogeneous population of myeloid progenitors that gave rise to all major myelo-erythroid cell lineages in vitro

Next, we sought to elucidate the differentiation potential of the putative progenitors associated with the adult mouse brain. To this end, we performed methylcellulose-based CFU assays, in which colonies of various myeloid lineage cells can be distinguished by morphology (Table S1). Within 7 to 10 days of culture, diverse colony types developed, comprising one or multiple myeloid cell types (Figure 2A). The most prominent were CFU-granulocyte (CFU-G), CFU-macrophage (CFU-M), CFU-granulocyte/macrophage (CFU-GM), and burst-forming units-erythroid (BFU-E). When comparing the CFU ratios derived from brain, blood, and BM, we found that the brain-associated pattern significantly differed from those found in blood and BM (Figure 2B). Conversely, cells from BM robustly gave rise to the same CFU ratios, irrespective of the sampling site (femur/tibia or skull). This observation supported the idea that the brain harbored an own population of progenitors. Also, applying the extended brain cell isolation protocol (enzymatic digestion and myelin removal) to BM progenitors did not alter their in vitro differentiation potential (Figure S4), suggesting that tissue processing did not introduce the differences observed. In comparison to blood and BM, brain homogenates displayed a more even distribution of CFU-G, CFU-M, CFU-GM, and BFU-E, with BFU-E being the most frequent colony type. Nevertheless, flow cytometric analysis of liquid cultures supplemented with monocyte/granulocyte-directing cytokines showed no difference in the frequency of monocytes and neutrophils produced by brain- or BM-derived progenitors (Figure S5A). Apart from the aforementioned CFUs, other colony types such as CFU-megakaryocyte (CFU-Mk) or mixed colonies comprising erythrocytes and megakaryocytes rarely derived from brain cell isolates (Figure 2C). As their cumulative frequency was <5%, these CFUs were not included in the ratio comparison. They demonstrated, however, that the brain-associated progenitor population had the potential to differentiate into all mature myeloid cell types in vitro, which was corroborated by immunostainings of F4/80, Ly6G, and GP1Bα following cytokine-induced differentiation in liquid cultures (Figure S5B).

Having confirmed the myelo-erythroid potential of brain-associated CFU-Cs, we tested whether these cells displayed the same immunophenotype as myeloid progenitors inside the BM. Hence, brain cell suspensions were successively split into various fractions by cell sorting and analyzed in CFU assays. We found that brain-derived CFU-Cs were exclusively contained within the CD45$^{+/lo}$ lineage marker (LIN$^-$) (CD5, TER-119, CD11B, 7-4, CD45R, GR.1) CD127$^-$ stem cell antigen-1 (SCA-1$^-$) c-KIT$^+$ fraction (Figure 2D), which is a phenotype reminiscent of myeloid progenitors in the BM.[50] This fraction could be further stratified based on differential expression of FcɣR and CD34 (Figure 2E), which identifies common myeloid progenitors (CMP), megakaryocyte-erythroid progenitors (MEP), and granulocyte-macrophage progenitors (GMP).[51] We validated our sorting approach with BM cells isolated from femora and tibiae (Figure 2F). As expected, MEPs almost exclusively gave rise to colonies of the erythroid branch (comprising erythrocytes and megakaryocytes), whereas the GMP fraction predominantly developed colonies of granulocytes and macrophages. CMPs gave rise to colonies of both myeloid branches, and colony size was often larger than in the other progenitor fractions. Importantly, progenitors within brain cell isolates could be split into the same subpopulations, which behaved comparably in methylcellulose-based CFU assays. Hence, adult mouse brain contained a hierarchy of myeloid progenitors, similar to those in adult BM.

3.4 | Brain-associated CFU-Cs derived from definitive hematopoiesis

During the embryonic period, YS-derived erythro-myeloid progenitors (EMP) and their progeny are invading the developing brain to establish the microglia pool.[52-54] It is conceivable that some EMPs persisted into early adulthood and gave rise to colonies in CFU assays. To elaborate the origin of brain-associated progenitors, we analyzed clonogenic cells in the Flt3^{Cre} model, which stably labels fetal and adult HSC-derived multipotent hematopoietic progenitors and their progeny (Figure 3A).[55,56] Single cell suspensions were prepared from blood, skull BM, and brain of Flt3^{Cre}:R26$^{mT/mG}$ mice. Flow cytometric analysis demonstrated the functionality of the model, as 91.4% ± 4.9% of CD45$^+$ leukocytes in blood and 89.4% ± 5.3% of CD45$^+$ cells in skull BM were Flt3^{Cre} GFP$^+$, indicating their descendance from HSCs. Conversely, YS-derived microglia lacked the cre-mediated recombination and did not express GFP (Figure 3B). CFU assays were performed with cell suspensions from skull BM and brain. Eventually, the fluorescence of individual colonies was assessed (Figure 3C). In accordance with the flow cytometry data, 86% ± 10% of BM-derived colonies were GFP$^+$. The proportion of GFP$^+$ colonies was lower when analyzing brain cells, yet the vast majority indicated cre-mediated recombination (68% ± 8%). Thus, even if it cannot be excluded that some Flt3-independent EMPs persisted in the brains of adult mice, most brain-derived colonies showed a history of Flt3 expression, pointing to their descendance from late fetal or adult HSCs.

To test whether brain-associated progenitors were replaced by the progeny of adult HSCs in the BM, we created chimeric mice by transplanting BM from B6.ubc-GFP animals into wild-type hosts. In a preliminary experiment, we used whole-body irradiation of the recipient to allow for the efficient engraftment of donor HSCs. Following this procedure, all brain-derived colonies in CFU assays were GFP$^+$ and therefore of donor origin (data not shown). However, whole-body irradiation does not only clear the BM niche, but also
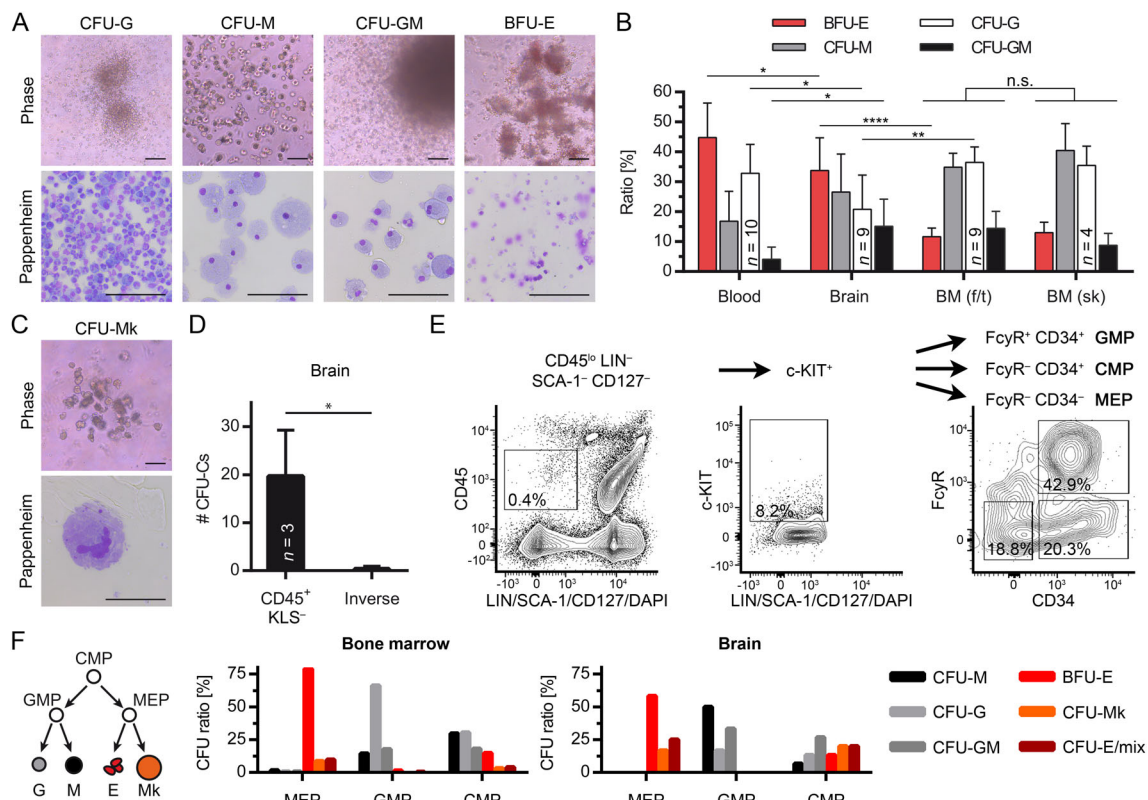
FIGURE 2 Brain-associated colony-forming units-culture (CFU-C) comprised a heterogeneous population of myeloid progenitors that gave rise to all major myelo-erythroid cell lineages in vitro. A, Various myelo-erythroid CFUs including CFU-G (granulocyte), CFU-M (macrophage), CFU-GM (granulocyte-macrophage), and BFU-E (burst-forming unit-erythroid) were identified in methylcellulose-based CFU assays of mouse brain cells (day 7-9) and verified via Pappenheim staining. Scale bars = 100 μm. B, Adult brain harbored a unique pattern of CFUs in comparison to BM and mixed peripheral blood. Data represent mean + SD and were pooled from at least two independent experiments including a total of n = 9-10 mice. BM, bone marrow; f/t, femur/tibia; sk, skull. Statistical analysis was performed using ordinary two-way ANOVA with Tukey's multiple comparisons test. *P < .05, **P < .01, ****P < .0001; n.s., nonsignificant. C, CFU-Mk (megakaryocyte) were rarely detected in brain cell isolates and verified via Pappenheim staining. Scale bars = 100 μm. D, Brain-derived CFU-Cs were exclusively contained within the CD45$^+$ LIN$^-$ (CD5, TER-119, CD11B, 7-4, CD45R, GR.1) SCA-1$^-$ c-KIT$^+$ (= CD45$^+$ KLS$^-$) population. Brain homogenates from adult mice were successively sorted into various cell fractions and their CFU-C content was analyzed in collagen-based CFU assays at day 7 of culture. Shown is the absolute number of colonies that developed within the CD45$^+$ KLS$^-$ fraction (or parts of the complete phenotype) vs the cumulative number of colonies found in all inverse populations. Data represent mean + SD and were pooled from three independent experiments. Statistical analysis was performed using an unpaired t test. *P < .05. E, Gating strategy to sort CD45^{lo} LIN$^-$ SCA-1$^-$ CD127$^-$ c-KIT$^+$ myeloid progenitors from brain or BM isolates (representative plots of brain cells are depicted), which were further divided into FcyR$^+$ CD34$^+$ granulocyte-macrophage progenitors (GMP), FcyR$^-$ CD34$^+$ common myeloid progenitors (CMP) and FcyR$^-$ CD34$^-$ megakaryocyte-erythrocyte progenitors (MEP). F, Brain-derived CFU-Cs constituted a hierarchy of myeloid progenitors as found in the BM (see simplified scheme on the left). Brain and BM cells were sorted into GMP, CMP, and MEP fractions as described in (E) and corresponding CFU types were analyzed in methylcellulose-based CFU assays at day 7. The myeloid progenitor phenotype (CD45$^+$ LIN$^-$ SCA-1$^-$ c-KIT$^+$) of brain CFU-Cs was verified in three independent experiments. Final sorting into GMPs, CMPs, and MEPs was performed once. G, granulocyte; M, macrophage; E, erythrocyte; Mk, megakaryocyte

leads to unspecific tissue damage,[57] opening of the blood-brain barrier,[58,59] and facilitates engraftment of HSPCs into the CNS.[19,20,22]

To exclude an artificial replacement of brain-associated progenitors after whole-body irradiation, we made use of a more gentle BM transplantation protocol, which was published recently.[34] Preconditioning in this model relies on the i.v. injection of αCD45 antibody, coupled to the ribosome-inactivating toxin saporin (CD45-SAP). Due to its high specificity, this technique should not suffer from the disadvantages mentioned above. Most importantly, it should preserve HSPCs behind the blood-brain or blood-arachnoid barrier.

This was supported by our cell sorting experiments, which had demonstrated that at least part of the brain-associated progenitor population was not accessible to intravenous anti-CD45 antibody (Figure 1E).

Compared to BM transfer after whole-body irradiation, chimerism developed more slowly in the CD45-SAP model and in our hands only reached around 50% in the blood myeloid compartment 15 weeks after transplantation (Figure 3D). At 7 and 15 weeks after transfer of B6.ubc-GFP BM, CFU assays were performed with cells from BM, blood, spleen, and brain. Developing colonies were assessed for GFP fluorescence via microscopy. In accordance with the myeloid blood
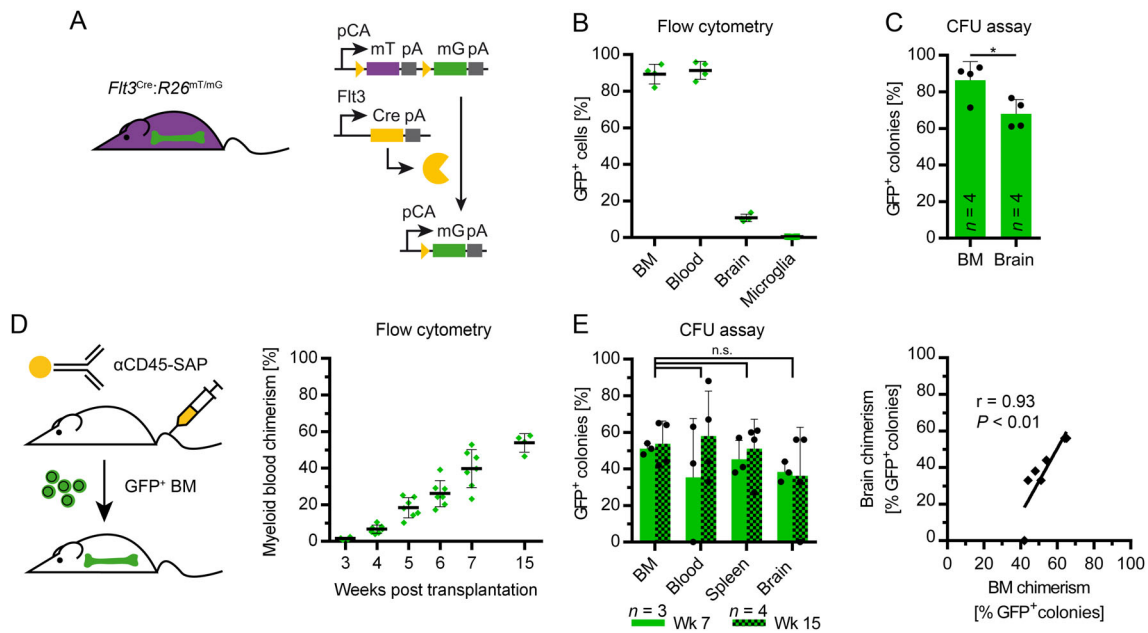
FIGURE 3 Brain-associated colony-forming units-culture (CFU-C) derived from hematopoietic stem cells (HSCs) in adult bone marrow (BM). A, Principle of tracing Flt3^{+} cell progeny in Flt3[Cre]:R26[mT/mG] mice by switch of reporter expression. PCA, chicken β-actin promoter; mT, membrane-targeted tomato; mG, membrane-targeted GFP; pA, polyadenylation sequence. B, The Flt3[Cre] model distinguishes between different cell ontogenies. HSC-derived hematopoietic (CD45^{+}) cells in BM and blood carry the cre-mediated recombination and therefore express GFP, in contrast to YS-derived CD45^{lo} CD11b^{+} microglia in the CNS. C, Brain-derived hematopoietic colonies had a history of Flt3 expression. Single cell suspensions were prepared from skull BM and brain of Flt3[Cre]:R26[mT/mG] mice and analyzed in collagen-based CFU assays. Colony fluorescence was examined at day 7 of culture. Data represent mean ± SD and were pooled from two independent experiments including a total of n = 4 mice. Statistical analysis was performed using a paired t test. *P < .05. D, Generation of BM chimeras. BM cells from B6.ubc-GFP mice were transplanted into WT recipients that had been preconditioned via i.v. injection of αCD45 antibody conjugated to saporin (CD45-SAP). Development of myeloid blood chimerism (% GFP^{+} cells among CD45^{+} CD11b^{+} myeloid blood cells) was monitored via flow cytometry. Data represent mean ± SD and derived from one experiment including n = 4-7 mice per time point. E, Brain-associated CFU-Cs were replaced by transplanted BM. Chimeric mice were generated as described in (D) and sacrificed 7 and 15 weeks post BM transplantation. The percentage of GFP[+] colonies was determined in collagen-based CFU assays prepared from BM, blood, spleen, and brain. Colony fluorescence was analyzed at day 7 of culture. Data represent mean + SD and derived from one experiment including n = 3-4 mice per time point. Statistical comparisons were performed using ordinary one-way ANOVA with Tukey's multiple comparisons test. n.s., nonsignificant. Correlation between BM and brain chimerism was calculated using nonparametric Spearman correlation

chimerism, around 50% of colonies that developed from BM were GFP[+] (Figure 3E). CFU-Cs from blood, spleen, and brain behaved similarly, irrespective of the time point of analysis. Thus, brain-associated progenitors were replaced by transplanted cells in the same manner as recipient BM. Chimerism of brain-associated progenitors correlated with chimerism in the BM, accordingly (Spearman correlation, r = 0.93, P < .01).

3.5 | Brain-associated CFU-Cs predominantly resided in the LM

To learn more about the anatomic location of brain-associated myeloid progenitors, we tested different tissue fractions in CFU assays. We dissected the brain into a pooled fraction of hippocampus and olfactory bulbs, and isolated the choroid plexus from the remaining tissue. Additionally, thin slices were collected from the dorsal and ventral surfaces of the cerebrum to enrich for the LM. The dural

meninges, which usually adhered to the skull during dissection, were not analyzed. Cells from hippocampus and olfactory bulbs rarely gave rise to colonies in CFU assays (0.2 ± 0.3 per 10[5] cells) and no CFU-Cs were detected in the choroid plexus. Conversely, CFU-Cs were significantly enriched within the meningeal fraction (4 ± 4.6 per 10[5] cells), whereas only 0.3 ± 0.4 CFU-Cs per 10[5] cells were observed in the remaining cerebrum. Within the cerebellum, from which the meninges had not been sliced off, 0.8 ± 0.8 CFU-Cs per 10[5] cells were detected (data not shown).

To confirm the presence of myeloid progenitors in the LM, meningeal whole-mounts, which include the dura as well as parts of the arachnoid mater,[35,60] were stained for the progenitor marker c-KIT (Figure 4B). Next to many c-KIT[+] avidin^{+} mast cells, which were scattered throughout the meninges (121.9 ± 27.7 cells per mm[2]), we found a rare population of c-KIT[+] avidin^{−} cells (2 ± 1.6 cells per mm[2]). These cells were usually smaller and more round-shaped than neighboring pleomorphic mast cells. They also showed stronger c-KIT expression, supporting their progenitor phenotype.
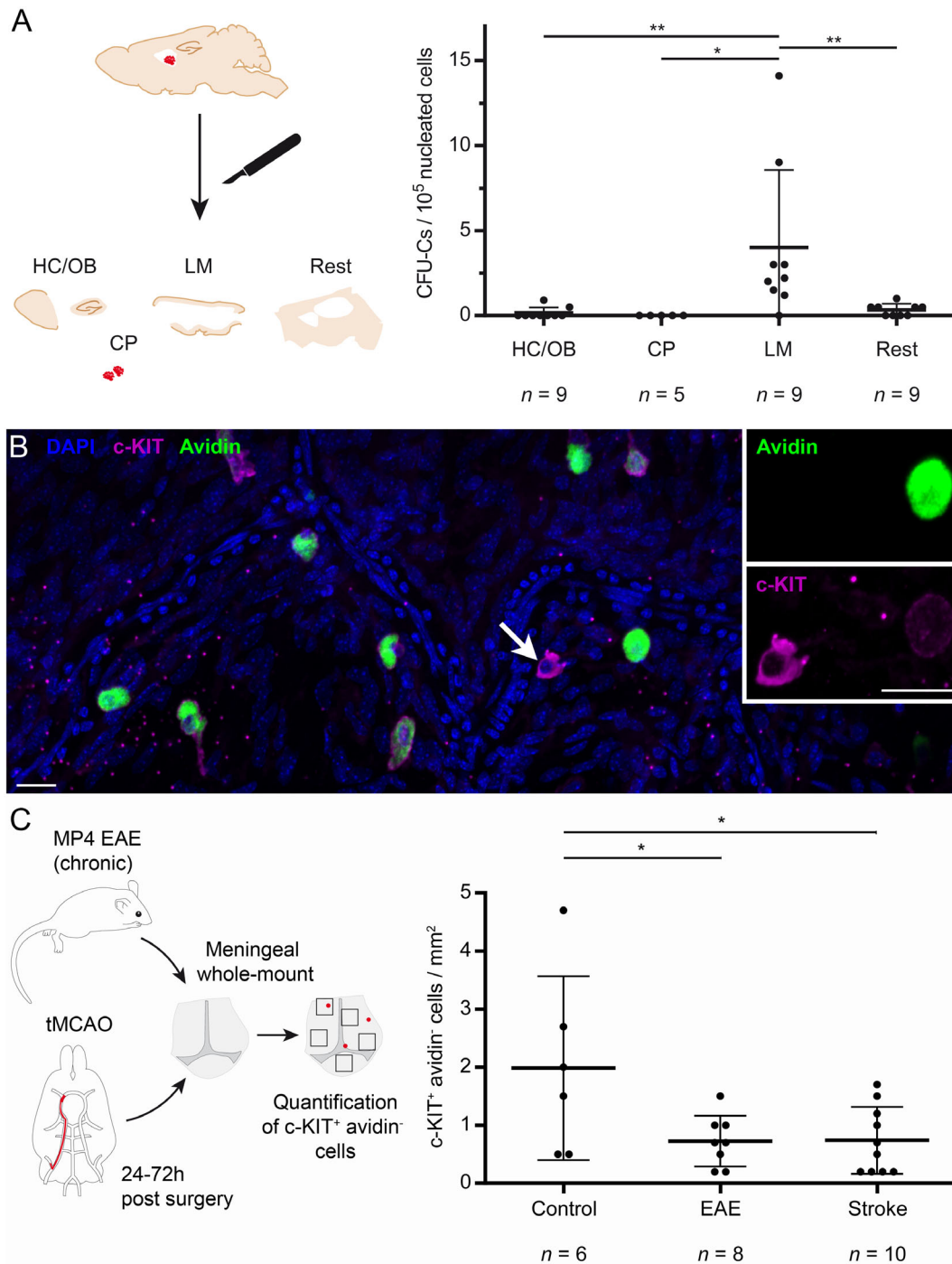
FIGURE 4 Brain-associated colony-forming units-culture (CFU-C) predominantly resided in the LM. A, Brain-associated CFU-Cs were enriched in the LM. The brain of adult mice was split into different fractions (shown on the left), including hippocampus and olfactory bulbs (HC/OB), choroid plexus (CP), leptomeninges (LM), and remaining cerebral tissue (Rest), all of which were analyzed in collagen-based CFU assays. Quantification of derived colonies is shown on the right. Data represent mean ± SD and were pooled from at least two independent experiments including a total of n = 5-9 mice. Statistics were performed using ordinary one-way ANOVA with Tukey's multiple comparisons test. *P < .05, **P < .01. B, Next to c-KIT$^+$ avidin$^+$ mast cells, rare avidin$^-$ cells (arrow) were found in meningeal (dura mater + arachnoid mater) whole-mounts strongly expressing the progenitor marker c-KIT. Scale bars = 20 μm. C, Meningeal c-KIT+ avidin$^-$ cells were diminished during CNS disease. Meningeal whole-mounts were prepared from control and chronic MP4 EAE mice as well as animals that had been subjected to transient middle cerebral artery occlusion (tMCAO). Tissue was stained with anti-c-KIT antibody and avidin-FITC. Eventually, c-KIT$^+$ avidin$^-$ cells were counted manually in confocal images selected at random. Data represent mean ± SD and derived from one experiment including n = 6-10 mice per group. Statistics were performed using ordinary one-way ANOVA with Tukey's multiple comparisons test. *P < .05

3.6 | Single cell RNA (scRNA) sequencing of cells derived from the brain surface

In an attempt to further characterize the phenotype and function of meningeal progenitors, scRNA sequencing was performed. To this end, tissue fragments were scraped from the outside of the cerebrum to acquire a sample enriched for meningeal cells, which was enzymatically digested (Figure S6A). To further enrich this sample for progenitors, recovered cells were treated with KIT-microbeads and sorted via MACS. Flow cytometric analysis showed an increase of KIT+ cells in the preparation from <1% to around 30% by this procedure. Eventually, the enriched cell preparation was used for single cell RNA sequencing. A total of 2141 cells with >500 sequenced genes per cell were included in the analysis. Unsupervised clustering produced five different clusters (Figure S6B), which differed in their gene expression profile (Figure S6C). Cluster 1, the largest cluster, was not characterized by any clear marker gene and was identified as a "mixed" cluster of different cell types that could not be further resolved. However, as *ptprc* and *csf1r* were mainly expressed in this cluster, it was deduced that it at least included hematopoietic cells and microglia (Figure S6D). Cells in cluster 2 expressed transcripts such as *Snhg1*, *Meg3*, *Nav2*, *Syne*, and *Gria3* and were identified as neurons, whereas cluster 3 cells predominantly expressed *1500015O10Rik*, *enpp2*, *kl*, *ttr*, *sostdc1*, *igfbp2*, and *prlr*, marking them as astro-ependymal cells. Cluster 4 was comprised of vascular cells expressing transcripts such as *cldn5*, *ly6a*, *flt1*, *ly6c1*, *kdr*, *vcam1*, and *vwf*. Cluster 5, the smallest cluster, was connected to the hematopoietic/myloid cluster 1. It was characterized by many transcripts of ribosomal protein genes, the myeloid transcription factor *irf8* as well as MHCII-associated (*h2-ab1*, *cd74*, *h2-aa*, *h2-eb1*) and granulocytic transcripts (*s100a8*, *s100a9*, *elane*, *ngp*, *camp*). Cluster 5 was the most promising cluster to harbor myeloid progenitors. However, due to the low purity of the sequenced cells in terms of KIT expression and the high contamination with nonhematopoietic cell types, it could not be resolved whether this cluster was merely a mix of mature blood cell types such as granulocytes and dendritic cells. Importantly, cluster 5 was also characterized by the oncogenes *fos* and *junb*, which have been described as tissue dissociation-induced immediate early genes (IEG). Hence, we cannot exclude the possibility that this cluster may be an artifact resulting from enzymatic treatment.

3.7 | Meningeal c-KIT+ avidin− cells were diminished during EAE and ischemic stroke

In a final set of experiments, we set out to test whether CNS inflammation affects the presence of progenitors in the meningeal compartment. Hence, c-KIT+ avidin− cells were quantified in meningeal whole-mounts prepared from chronic MP4-immunized EAE mice or animals that had been subjected tMCAO, a model of ischemic stroke (Figure 4C). Progenitor-like cells were consistently diminished to around 50% of control levels in both disease models.

4 | DISCUSSION

Here, we describe a heterogeneous population of brain-associated myeloid progenitors, which include at least CMPs, MEPs, and GMPs. The progenitors predominantly resided in the LM of adult mice and gave rise to all major myelo-erythroid cell lineages in vitro. Their frequency was found to be 7 ± 4 per 10^5 isolated cells. This number is comparable to previous studies (Table S3) and leads to an estimated total number of 40 to 70 progenitors per mouse brain (parenchyma + choroid plexus + LM).

Brain-derived myeloid progenitors showed a differentiation bias toward the erythroid lineage in vitro, which matches earlier observations in spleen colony forming assays.[24] This underlined that the cells did not constitute a mere contamination by skull BM, which rarely gave rise to erythroid colonies under the same conditions. However, removal of APC+ cells following intravenous injection of αCD45-APC antibody eliminated about 50% of clonogenic cells from the brain homogenate, suggesting their localization inside of blood vessels. This was somewhat surprising, as intravascular progenitors were expected to only account for ∼0.15 colonies per 10^5 CNS-derived cells, based on the average frequency of circulating progenitors in peripheral blood (4 ± 3 CFU-Cs per 10^5 nucleated cells) and the mean residual leukocyte count in brain tissue after PBS perfusion ($2.3\% \pm 1\%$ IV-CD45+ cells). It is possible that progenitors were attached to the blood vessel endothelium or located inside the CNS barriers at the time of injection, where they could still be labeled by intravenous antibodies. Nevertheless, the presence of intravascular progenitors would explain the similar in vitro potentials of brain- and blood-derived precursors, even though the overall colony patterns significantly differed. Adapting the αCD45 injection scheme in order to additionally stain the majority of skull BM cells did not lower the frequency of CFU-Cs in the IV-CD45− fraction any further. Therefore, the remaining progenitors did not represent a spill from BM, but were rather located behind the blood-brain or blood-arachnoid barriers, where they could not be reached by intravenous antibodies. A contamination by dural cells can also be excluded, as i.v. injected antibodies are expected to penetrate through the fenestrated endothelium of dural blood vessels in the same manner as through fenestrated BM sinusoids.[38]

When Alliot et al observed rapidly proliferating cells in cultures from mouse brain almost 30 years ago, they termed them "microglia progenitors," as their experimental approach specifically examined cells that differentiated into a macrophage-like phenotype in response to M-CSF stimulation.[25] They also suggested the progenitors to originally derive from the YS and to persist into adulthood.[52] Since then, knowledge on microglia development and maintenance has expanded considerably. Although the YS origin of microglia has been confirmed, terminally differentiated microglia as well as other macrophage populations inside the CNS have been shown to self-renew independently of infiltrating or resident progenitors.[41,43,61] Still, we did not exclude the possibility of some YS-derived microglia progenitors persisting in the adult CNS, especially as the erythroid-tended colony pattern of CNS-associated progenitors was reminiscent of EMPs.[62] Hence, we performed CFU assays with brain suspensions of *Flt3*Cre:

$R26^{mT/mG}$ mice, which label fetal and adult HSC-derived multipotent hematopoietic progenitors and their progeny via GFP expression.[42,43] YS-derived EMPs as well as EMP-derived cells do not express *Flt3* and so are not tagged in this model.[43,48] As the majority of colonies that developed from $Flt3^{Cre}:R26^{mT/mG}$ brain suspensions expressed GFP, it can be concluded that the progenitors descent from late fetal or adult HSCs, but not from the YS. The myeloid progenitors are therefore not involved in microglia maintenance, as microglia have been shown to self-renew independently of HSC-derived cells and remain unlabeled in $Flt3^{Cre}$ mice at least until 1 year of age.[40,56] Concurrently, this result confirmed that mature microglia were not responsible for colony-formation in vitro, which we also demonstrated in CFU assays with purely sorted $Iba1^+$ cells.

Previous analyses of anemic W^f/W^f mice and parabionts have suggested that there might be no or only minor exchange between the BM and the brain-associated progenitor compartment.[11,24] However, in CD45-SAP-induced BM chimeras, brain-associated progenitors were replaced by donor cells to the same extent as progenitors in blood, spleen, and BM. It is important to note that treatment with CD45-SAP immunotoxin is not expected to compromise CNS integrity[34] and therefore should spare cells that are located behind the blood-brain or blood-arachnoid barrier at the time of injection. This is supported by our cell sorting experiments showing that part of the brain-associated progenitor population was protected from intravenous antibodies. Thus, in CD45-SAP-induced BM chimeras, myeloid progenitors in the CNS niche were most likely physiologically replaced by BM-derived cells that traffic throughout the body, as it has been shown for other organs.[11]

Although clonogenic cells have been observed in the adult CNS before, little is known about their anatomic location. Nataf et al described myeloid progenitors in the rat choroid plexus, which we could not confirm in mice.[63] Alliot et al found a relatively high frequency of cells with hematopoietic progenitor characteristics in adult forebrain and brainstem ($\sim$13-14 per 10^5 cells), whereas they were less abundant in the cerebellum ($\sim$ 3 per 10^5 cells).[25] In principle, this conforms to our results. However, the authors stated to have carefully removed the meninges prior to cell isolation.[25] Conversely, own fractionation experiments showed that brain-associated myeloid progenitors predominantly resided in the LM. In accordance with these findings, we observed rare c-KIT$^+$ cells in dural/arachnoid whole-mounts, which could be clearly distinguished from mature c-KIT$^+$ avidin$^+$ mast cells. Recent studies employing high-dimensional mass and fluorescence cytometry as well as single cell sequencing have revealed a broad spectrum of immune cells in the healthy CNS, especially at its borders.[64-66] It seems likely that myeloid progenitors are intermingled with these CNS-associated immune populations. Intriguingly, in the context of the exhaustive analyses cited above, Korin et al detected a cohort of CD45^{lo} "undefined cells" in the CNS. These cells lacked myeloid differentiation markers, but partly expressed CXCR4, an important chemokine receptor on HSPCs.[65,67] It is plausible that the herein described CD45^{lo} LIN$^-$ progenitors are hidden inside this "undefined" population.

Overall, future studies including, for example, in situ hybridization will have to be performed to further narrow down the exact localization of the progenitor population and to determine whether they are solely associated with the LM or also reside within the brain parenchyma.

Likewise, more studies are necessary to elucidate the functional role of the progenitor population. Although our initial attempt to further characterize the cells by scRNA sequencing provided valuable insights into the composition of the meningeal preparations and may therefore serve as a foundation to improve marker-based enrichment of progenitors, we were not able to identify a definite progenitor cluster, illustrating the challenge of analyzing such a rare cell population. Nevertheless, overcoming this challenge might be worthwhile, as it is tempting to speculate that the existence of leptomeninx-associated myeloid progenitors may have important implications for the field of neuroimmunology. It has been shown that HSPCs constantly leave and reenter the BM, circulate in the blood, and visit various tissues before returning to the blood via draining lymphatics.[11] On their journey, HSPCs sense pathogens via Toll-like receptors[11,12] and react with proliferation, differentiation into myeloid cells,[11,12] and cytokine production.[18,68] Because of their plasticity and high proliferative potential, even a small number of progenitors might be able to significantly shape local immune responses. In CFU assays, this is demonstrated by the ability of a single progenitor cell to produce thousands of daughter cells over the course of a few days. It is therefore conceivable that hematopoietic progenitors also exert an effective surveillance function at the CNS border. Correspondingly, the lower frequencies of meningeal c-KIT$^+$ avidin$^-$ cells, which we observed during EAE and ischemic stroke, may point toward an activation of leptomeninx-associated progenitors in response to CNS disease, leading to their differentiation (and loss of c-KIT-expression) and/or migration into the brain parenchyma. In that case, the precursors' direct contact to local cues might even result in the generation of innate immune cells that are specifically adapted to the prevailing brain environment, as recent studies have shown that "trained immunity" is already formed on the level of the HSPC compartment.[69,70] A meningeal localization would be optimally suited for such tasks, because interstitial and cerebrospinal fluid washes macromolecules from all over the CNS into the subarachnoid space prior to drainage into meningeal lymphatics.[71,72]

CONFLICT OF INTEREST

The authors declared no potential conflicts of interest.

AUTHOR CONTRIBUTIONS

DATA AVAILABILITY STATEMENT

ORCID

Philipp Wörsdörfer https://orcid.org/0000-0003-3398-3229
Stefanie Kuerten https://orcid.org/0000-0001-6119-605X

REFERENCES

1. Orkin SH, Zon LI. Hematopoiesis: an evolving paradigm for stem cell biology. *Cell*. 2008;132:631-644.
2. Wright DE. Physiological migration of hematopoietic stem and progenitor cells. *Science (80-)*. 2001;294:1933-1936.
3. Spencer RP, Pearson HA. The speen as a hematological organ. *Semin Nucl Med*. 1975;5:95-102.
4. Cardier JE, Barberá-Guillem E. Extramedullary hematopoiesis in the adult mouse liver is associated with specific hepatic sinusoidal endothelial cells. *Hepatology*. 1997;26:165-175.
5. McKinney-Freeman SL, Jackson KA, Camargo FD, et al. Muscle-derived hematopoietic stem cells are hematopoietic in origin. *Proc Natl Acad Sci USA*. 2002;99:1341-1346.
6. Massberg S, Schaerli P, Knezevic-Maramica I, et al. Immunosurveillance by hematopoietic progenitor cells trafficking through blood, lymph, and peripheral tissues. *Cell*. 2007;131:994-1008.
7. Fu J, Zuber J, Martinez M, et al. Human intestinal allografts contain functional hematopoietic stem and progenitor cells that are maintained by a circulating pool. *Cell Stem Cell*. 2019;24:227-239.e8.
8. Zlotoff DA, Bhandoola A. Hematopoietic progenitor migration to the adult thymus. *Ann N Y Acad Sci*. 2011;1217:122-138.
9. Montfort MJ, Olivares CR, Mulcahy JM, Fleming WH. Adult blood vessels restore host hematopoiesis following lethal irradiation. *Exp Hematol*. 2002;30:950-956.
10. Psaltis PJ, Harbuzariu A, Delacroix S, et al. Identification of a monocyte-predisposed hierarchy of hematopoietic progenitor cells in the adventitia of postnatal murine aorta. *Circulation*. 2012;125:592-603.
11. Massberg S, Schaerli P, Knezevic-Maramica I, et al. Immunosurveillance by hematopoietic progenitor cells trafficking through blood, lymph, and peripheral tissues. *Cell*. 2007;131:994-1008.
12. Nagai Y, Garrett KP, Ohta S, et al. Toll-like receptors on hematopoietic progenitor cells stimulate innate immune system replenishment. *Immunity*. 2006;24:801-812.
13. Megías J, Yáñez A, Moriano S, O'Connor JE, Gozalbo D, Gil ML. Direct toll-like receptor-mediated stimulation of hematopoietic stem and progenitor cells occurs in vivo and promotes differentiation toward macrophages. *Stem Cells*. 2012;30:1486-1495.
14. Megías J, Martínez A, Yáñez A, Goodridge HS, Gozalbo D, Gil ML. TLR2, TLR4 and Dectin-1 signalling in hematopoietic stem and progenitor cells determines the antifungal phenotype of the macrophages they produce. *Microbes Infect*. 2016;18:354-363.
15. Si Y, Tsou CL, Croft K, Charo IF. CCR2 mediates hematopoietic stem and progenitor cell trafficking to sites of inflammation in mice. *J Clin Invest*. 2010;120:1192-1203.
16. Baldridge MT, King KY, Goodell MA. Inflammatory signals regulate hematopoietic stem cells. *Trends Immunol*. 2011;32:57-65.
17. Takizawa H, Regoes RR, Boddupalli CS, Bonhoeffer S, Manz MG. Dynamic variation in cycling of hematopoietic stem cells in steady state and inflammation. *J Exp Med*. 2011;208:273-284.
18. Allakhverdi Z, Delespesse G. Hematopoietic progenitor cells are innate Th2 cytokine-producing cells. *Allergy*. 2012;67:4-9.
19. Capotondo A, Milazzo R, Garcia-Manteiga JM, et al. Intra-cerebroventricular delivery of hematopoietic progenitors results in rapid and robust engraftment of microglia-like cells. *Sci Adv*. 2017;3:e1701211.
20. Capotondo A, Milazzo R, Politi LS, et al. Brain conditioning is instrumental for successful microglia reconstitution following hematopoietic stem cell transplantation. *Proc Natl Acad Sci USA*. 2012;109: 15018-15023.
21. Kierdorf K, Katzmarski N, Haas C a, et al. Bone marrow cell recruitment to the brain in the absence of irradiation or parabiosis bias. *PLoS One*. 2013;8:e58544.
22. Ajami B, Bennett JL, Krieger C, McNagny KM, Rossi FMV. Infiltrating monocytes trigger EAE progression, but do not contribute to the resident microglia pool. *Nat Neurosci*. 2011;14:1142-1149.
23. Mocco J, Afzal A, Ansari S, et al. SDF1-A facilitates Lin-/Sca1+ cell homing following murine experimental cerebral ischemia. *PLoS One*. 2014;9:e85615.
24. Bartlett PF. Pluripotential hemopoietic stem cells in adult mouse brain. *Proc Natl Acad Sci USA*. 1982;79:2722-2725.
25. Alliot F, Lecain E, Grima B, Pessac B. Microglial progenitors with a high proliferative potential in the embryonic and adult mouse brain. *Proc Natl Acad Sci USA*. 1991;88:1541-1545.
26. Asakura A, Rudnicki MA. Side population cells from diverse adult tissues are capable of in vitro hematopoietic differentiation. *Exp Hematol*. 2002;30:1339-1345.
27. Mazo IB, Gutierrez-Ramos J-C, Frenette PS, Hynes RO, Wagner DD, von Andrian UH. Hematopoietic progenitor cell rolling in bone marrow microvessels: parallel contributions by endothelial selectins and vascular cell adhesion molecule 1. *J Exp Med*. 1998;188:465-474.
28. Hirasawa T, Ohsawa K, Imai Y, et al. Visualization of microglia in living tissues using Iba1-EGFP transgenic mice. *J Neurosci Res*. 2005;81: 357-362.
29. Benz C, Martins VC, Radtke F, Bleul CC. The stream of precursors that colonizes the thymus proceeds selectively through the early T lineage precursor stage of T cell development. *J Exp Med*. 2008;205: 1187-1199.
30. Muzumdar MD, Tasic B, Miyamichi K, et al. A global double-fluorescent Cre reporter mouse. *Genesis*. 2007;45:418-426.
31. Schaefer BC, Schaefer ML, Kappler JW, Marrack P, Kedl RM. Observation of antigen-dependent CD8+ T-cell/dendritic cell interactions in vivo. *Cell Immunol*. 2001;214:110-122.
32. Jung S, Aliberti J, Graemmel P, et al. Analysis of fractalkine receptor CX3CR1 function by targeted deletion and green fluorescent protein reporter gene insertion. *Mol Cell Biol*. 2002;20:4106-4114.
33. National Research Council. *Guide for the Care and Use of Laboratory Animals*. 8th ed. Washington, DC: National Academies Press; 2011.
34. Palchaudhuri R, Saez B, Hoggatt J, et al. Non-genotoxic conditioning for hematopoietic stem cell transplantation using a hematopoietic-cell-specific internalizing immunotoxin. *Nat Biotechnol*. 2016;34:738-745.
35. Louveau A, Smirnov I, Keyes TJ, et al. Structural and functional features of central nervous system lymphatic vessels. *Nature*. 2015;523: 337-341.
36. Kuerten S, Lichtenegger FS, Faas S, Angelov DN, Tary-Lehmann M, Lehmann PV. MBP-PLP fusion protein-induced EAE in C57BL/6 mice. *J Neuroimmunol*. 2006;177:99-111.
37. Langhauser F, Casas AI, Dao VTV, et al. A diseasome cluster-based drug repurposing of soluble guanylate cyclase activators from smooth muscle relaxation to direct neuroprotection. *Npj Syst Biol Appl*. 2018; 4:8.

38. Braeuninger S, Kleinschnitz C, Nieswandt B, et al. Focal cerebral ischemia. *Methods Mol Biol*. 2012;788:29-42.

39. Schindelin J, Arganda-Carreras I, Frise E, et al. Fiji: an open-source platform for biological-image analysis. *Nat Methods*. 2012;9:676-682.

40. Goldmann T, Wieghofer P, Joana M, et al. Origin, fate and dynamics of macrophages at central nervous system interfaces. *Nat Immunol*. 2016;17:797-805.

41. Prinz M, Erny D, Hagemeyer N. Ontogeny and homeostasis of CNS myeloid cells. *Nat Immunol*. 2017;18:385-392.

42. Elmore MRP, Najafi AR, Koike MA, et al. Colony-stimulating factor 1 receptor signaling is necessary for microglia viability, unmasking a microglia progenitor cell in the adult brain. *Neuron*. 2014;82: 380-397.

43. Huang Y, Xu Z, Xiong S, et al. Repopulated microglia are solely derived from the proliferation of residual microglia after acute depletion. *Nat Neurosci*. 2018;21:530-540.

44. Bruttger J, Karram K, Wörtge S, et al. Genetic cell ablation reveals clusters of local self-renewing microglia in the mammalian central nervous system. *Immunity*. 2015;43:92-106.

45. Terashima T, Nakae Y, Katagi M, Okano J, Suzuki Y, Kojima H. Stem cell factor induces polarization of microglia to the neuroprotective phenotype in vitro. *Heliyon*. 2018;4:e00837.

46. Wei S, Nandi S, Chitu V, et al. Functional overlap but differential expression of CSF-1 and IL-34 in their CSF-1 receptor-mediated regulation of myeloid cells. *J Leukoc Biol*. 2010;88:495-505.

47. Lin H, Lee E, Hestir K, et al. Discovery of a cytokine and its receptor by functional screening of the extracellular proteome. *Science (80-)*. 2008;320:807-811.

48. Suzumura A, Sawada M, Yamamoto H, Marunouchi T. Effects of colony stimulating factors on isolated microglia in vitro. *J Neuroimmunol*. 1990;30:111-120.

49. Ryg-Cornejo V, Ioannidis LJ, Hansen DS. Isolation and analysis of brain-sequestered leukocytes from plasmodium berghei ANKA-infected mice. *J Vis Exp*. 2013;71 6-13.

50. Mayle A, Luo M, Jeong M, Goodell MA. Mouse hematopoietic stem cell identification and analysis. *Cytometry*. 2013;83:27-37.

51. Akashi K, Traver D, Miyamoto T, Weissman IL. A clonogenic common myeloid progenitor that gives rise to all myeloid lineages. *Nature*. 2000;404:193-197.

52. Alliot F, Godin I, Pessac B. Microglia derive from progenitors, originating from the yolk sac, and which proliferate in the brain. *Dev Brain Res*. 1999;117:145-152.

53. Ginhoux F, Greter M, Leboeuf M, et al. Fate mapping analysis reveals that adult microglia derive from primitive macrophages. *Science*. 2010;330:841-845.

54. Kierdorf K, Erny D, Goldmann T, et al. Microglia emerge from erythromyeloid precursors via Pu.1- and Irf8-dependent pathways. *Nat Neurosci*. 2013;16:273-280.

55. Christensen JL, Weissman IL. Flk-2 is a marker in hematopoietic stem cell differentiation: a simple method to isolate long-term stem cells. *Proc Natl Acad Sci USA*. 2001;98:14541-14546.

56. Perdiguero EG, Klapproth K, Schulz C, et al. Tissue-resident macrophages originate from yolk-sac-derived erythro-myeloid progenitors. *Nature*. 2015;518:547-551.

57. Han W, Umekawa T, Zhou K, et al. Cranial irradiation induces transient microglia accumulation, followed by long-lasting inflammation and loss of microglia. *Oncotarget*. 2016;7:82305-82323.

58. Yoshida Y, Sejimo Y, Kurachi M, Ishizaki Y, Nakano T, Takahashi A. X-ray irradiation induces disruption of the blood-brain barrier with localized changes in claudin-5 and activation of microglia in the mouse brain. *Neurochem Int*. 2018;119:199-206.

59. Li YQ, Chen P, Haimovitz-Friedman A, Reilly RM, Wong CS. Endothelial apoptosis initiates acute blood-brain barrier disruption after ionizing radiation. *Cancer Res*. 2003;63:5950-5956.

60. Coles JA, Myburgh E, Brewer JM, McMenamin PG. Where are we? The anatomy of the murine cortical meninges revisited for intravital imaging, immunology, and clearance of waste from the brain. *Prog Neurobiol*. 2017;156:107-148.

61. Zhan L, Krabbe G, Du F, et al. Proximal recolonization by self-renewing microglia re-establishes microglial homeostasis in the adult mouse brain. *PLoS Biol*. 2019;17:e3000134.

62. McGrath KE, Frame JM, Fegan KH, et al. Distinct sources of hematopoietic progenitors emerge before HSCs and provide functional blood cells in the mammalian embryo. *Cell Rep*. 2015;11:1892-1904.

63. Nataf S, Strazielle N, Hatterer E, Mouchiroud G, Belin MF, Ghersi-Egea JF. Rat choroid plexuses contain myeloid progenitors capable of differentiation toward macrophage or dendritic cell phenotypes. *Glia*. 2006;54:160-171.

64. Mrdjen D, Pavlovic A, Hartmann FJ, et al. High-dimensional single-cell mapping of central nervous system immune cells reveals distinct myeloid subsets in health, aging, and disease. *Immunity*. 2018;48:1-16.

65. Korin B, Ben-Shaanan TL, Schiller M, et al. High-dimensional, single-cell characterization of the brain's immune compartment. *Nat Neurosci*. 2017;20:1300-1309.

66. Van Hove H, Martens L, Scheyltjens I, et al. A single-cell atlas of mouse brain macrophages reveals unique transcriptional identities shaped by ontogeny and tissue environment. *Nat Neurosci*. 2019;22:1021–1035.

67. Karpova D, Bonig H. Concise review: CXCR4/CXCL12 signaling in immature hematopoiesis—lessons from pharmacological and genetic models. *STEM CELLS*. 2015;33:2391-2399.

68. Allakhverdi Z, Comeau MR, Smith DE, et al. CD34+ hemopoietic progenitor cells are potent effectors of allergic inflammation. *J Allergy Clin Immunol*. 2009;123:472-478.

69. Kaufmann E, Sanz J, Dunn JL, et al. BCG educates hematopoietic stem cells to generate protective innate immunity against tuberculosis. *Cell*. 2018;172:176-190.e19.

70. Mitroulis I, Ruppova K, Wang B, et al. Modulation of myelopoiesis progenitors is an integral component of trained immunity. *Cell*. 2018; 172:147-161.e12.

71. Ma Q, Ineichen BV, Detmar M, Proulx ST. Outflow of cerebrospinal fluid is predominantly through lymphatic vessels and is reduced in aged mice. *Nat Commun*. 2017;8:1434.

72. Raper D, Louveau A, Kipnis J. How do meningeal lymphatic vessels drain the CNS? *Trends Neurosci*. 2016;39:581-586.

SUPPORTING INFORMATION

Additional supporting information may be found online in the Supporting Information section at the end of this article.